Gonbad Kavous University

Journal of New Approaches in Water Engineering and Environment

Online ISSN: 2981-0280

Homepage: https://nawee.gonbad.ac.ir

Assessing Soft Computing Techniques for River Suspended Sediment Estimation

Amir Moradinejad[1*], Abbas Parsaie [2], Seyed Ahmad Hosseini[3], Mahmoudreza Tabatabaei[4]

[1] Soil Conservation and Watershed Management Research Department, Markazi Agricultural and Natural Resources Research and Education Center, Arak, Agricultural Research Education & Extention Organization (AREEO). Arak, Iran.
[2]Department of Hydraulic Structures, Faculty of Water and Environmental Engineering, Shahid Chamran University of Ahvaz, Ahvaz, Iran.
[3]Department of River and Coastal Engineering, Soil Conservation and Watershed Management Institute, Agricultural Research Education & Extention Organization (AREEO), Tehran, Iran.
[4] Soil Conservation and Watershed Management Research Institute, Agricultural Research, Education and Extension Organization (AREEO), Tehran, Iran.

Article Info

Article type:

Research Article

Article history:
Received 01 April 2025
Revised 14 February 2025
Accepted 08 July 2025
Published online 14 June 2025

Keywords:
suspended load
fuzzy neural network
sedimentation
gene expression
support vector

ABSTRACT

Objective: Statistical and regression models are commonly used for this purpose, but they often yield inaccurate results due to the linear assumptions inherent in these approaches. Hydraulic models, while useful, cannot always be fully trusted due to their requirement for extensive data, the potential unavailability of required data, and the possibility of human errors leading to inaccuracies in sediment simulation. To overcome these challenges, data-driven methods—specifically a subset of soft computing techniques—can be employed.

Material and Methods: This study aims to evaluate and compare five methods for estimating the sediment load at the Pol Doab station on the Qarachai River in Markazi Province, Iran. The methods considered include the Adaptive Network-based Fuzzy Inference System (ANFIS), Support Vector Machine (SVM), Gene Expression Programming (GEP), Multivariate Adaptive Regression Splines (MARS), and the Group Method of Data Handling (GMDH). The performance of these models in simulating the sediment load of rivers was assessed, and the results were compared both among the five methods and with those obtained from the sediment rating curve.

Results and Discussion: The statistical indicators showed the following results for each method at the station:
For the SVR model: R^2=0.98R^2 = 0.98R^2=0.98, RMSE = 185, and MBE = -5.43. For the ANFIS model: R^2=0.79R^2 = 0.79R^2=0.79, RMSE = 24.3, and MBE = 1.9. For the GEP model: R^2=0.98R^2 = 0.98R^2=0.98, RMSE = 0.74, and MBE = 0.00047. In the next step, the best-performing patterns from the ANFIS, SVM, and GEP models were used as inputs for the GMDH model. The results indicated that the GMDH model demonstrated the highest performance, with R^2=0.99, 0.91, 0.98 R^2 = 0.99, 0.91, 0.98R^2=0.99, 0.91, 0.98, RMSE = 83, 24, 73 (tons per day), and MBE = 3.2, 1.8, 1.2 respectively.

Conclusion: The findings suggest that the GEP model, with R^2=0.98R^2 = 0.98R^2=0.98, RMSE = 0.74, and MBE = 0.00047, outperforms the SVM, ANFIS, and GMDH models to some extent. Moreover, the results demonstrate that all five data mining methods investigated in this study provide significantly better estimates than the traditional sediment rating curve.

*Corresponding author, Email: amir_24619@yahoo.com

Cite this article: Moradinejad, Amir., Parsaie, Abbas., Hosseini, Seyed Ahmad., Tabatabaei, Mahmoudreza. (2025). Assessing Soft Computing Techniques for River Suspended Sediment Estimation. *Journal of New Approaches in Water Engineering and Environment*, 4(2), 188-212. https://doi.org/10.22034/nawee.2025.514714.1147

Publisher: Gonbad Kavous University.
DOI: https://doi.org/ 10.22034/nawee.2025.514714.1147

1. Introduction

Sediment transport and sedimentation can lead to several negative consequences, including the formation of sediment islands within rivers, reduced storage capacity in reservoirs, and a shortened lifespan of dams. Sediment-laden flows can damage water infrastructure and agricultural lands, reduce the water-carrying capacity of waterways and transfer facilities, and alter the quality of drinking and agricultural water. As such, evaluating the amount of suspended sediment in rivers is crucial for the design and operation of water projects in water engineering. Estimating suspended sediment loads is important for various applications, including dam reservoir design, sediment and pollution transport in rivers, stable channel design, erosion and sedimentation assessment around bridge foundations, and watershed management (Melesse et al., 2011). Experts have proposed numerous relationships to estimate river suspended loads. However, due to the complex nature of sediment transport, experimental results often deviate from actual values, resulting in a lack of universally accepted models (Azamathulla et al., 2013). Estimating sediment load in rivers is a critical and practical aspect of water engineering studies and design projects. Sediment concentration can be determined using direct or indirect methods, though direct methods are often expensive and time-consuming. Several factors influence sediment transport, making its analysis challenging (Kisi et al., 2008). Statistical and regression models frequently produce inaccurate results due to their linear assumptions when applied to the complex phenomena of sediment transport. As such, these models cannot accurately represent sediment transport (Walling & Webb, 1988). Hydraulic models are also unreliable due to their high data requirements. Often, the required data are unavailable or inaccurate due to human error in sediment simulation. Given the data uncertainty and the complex, multi-variable nature of sediment transport, soft computing methods have become essential for estimating suspended sediment loads (Tayfur, 2012). As a result, researchers have sought alternative methods that do not rely on traditional equations. In this regard, artificial intelligence, which can model complex natural relationships with high flexibility, offers a promising approach. Today, fuzzy and neural intelligent systems are widely used in water engineering problems, including sedimentation, due to their ability to handle complex and nonlinear phenomena.

Numerous studies have been conducted around the world to investigate these methods. For instance, Kisi et al. (2008) assessed the performance of a neural-fuzzy adaptive inference system in estimating monthly suspended sediment loads for the Keulos and Salurkopru rivers in Turkey. Their results, which were compared with those of artificial neural network models and sediment rating curves, demonstrated that the neural-fuzzy adaptive inference system outperformed the other two methods. Eder et al. (2010) explored the effect of sedimentation on river suspended loads, showing that the sediment rating curve method had lower accuracy compared to other methods. Duan et al. (2015) applied the SPARROW method to model suspended sediment sources and transport within the Ishikari basin. Their study highlighted the sediment production and transport processes in the basin and demonstrated the method's applicability in water resources management. Sattari et al. (2016) compared the performance of the M5 tree model and support vector regression methods to the sediment rating curve for suspended sediment modeling in the Aharchai River. Their results showed that data mining methods outperformed the sediment rating curve, with the M5 tree model providing a simpler and more interpretable linear relationship. Beirandvand et al. (2022) assessed the effectiveness of various machine learning algorithms (e.g., GP-RBF, GP-PUK, RepTree, RF, and M5P models) for predicting river suspended load during low-water periods in the Kashkan watershed. Their findings indicated that the GP model incorporating both PUK and RBF kernels performed better than other models during periods of water scarcity and abundance, with the

GP-PUK model showing the best performance. Keshtegar et al. (2023) used soft computing methods to estimate river-suspended sediment in Pakistan, comparing the performance of RM5Tree models with Support Vector Regression (SVR), Artificial Neural Network (ANN), Multivariate Adaptive Regression Splines (MARS), the Sediment Scale Curve (SRC), and Response Surface Method (RSM) models. Their results showed that the RM5Tree model outperformed the other models, achieving a relative accuracy of 84.10%.

The settling of suspended sediments in rivers can reduce the river's cross-sectional area and alter its channel shape, thus diminishing habitats for aquatic animals (Adnan et al., 2022). Imamqolizadeh et al. (2015) evaluated soil cation exchange capacity using GEP and MARS gene expression programming models, comparing their performance to ANN and multiple linear regression models. Their results indicated that both GEP and MARS models provided reliable estimations. Adamowski et al. (2012) used the MARS model to predict floods in Himalayan sub-basins with limited data, finding that the MARS model outperformed a neural network in estimating floods. Yilmaz et al. (2018) used MARS models, an artificial bee colony algorithm, and an optimization algorithm to estimate the suspended sediment load of the Kuru River in Turkey, concluding that MARS provided the most accurate simulations. Sadegh Safar (2020) investigated the prediction of suspended sediment load using MARS and random forest models, showing that the MARS model was accurate in predicting suspended sediment loads. García et al. (2019) employed MARS and M5 models to simulate algae types that contribute to significant lake ecosystem degradation (García-Nieto et al., 2019).

MARS has emerged as an effective method for estimating suspended sediment load, especially compared to the traditional sediment rating curve. Alizamir et al. (2020) and Mostafa et al. (2023) compared hybrid random vector functional link (RVFL) and hybrid ANFIS models to standalone models in evapotranspiration calculations, concluding that hybrid RVFL and ANFIS models provide robust approaches. Similarly, Ikram et al. (2023) developed a hybrid model combining long short-term memory (LSTM) and a conventional neural network (CNN) for water temperature prediction, showing that the hybrid model outperforms standalone deep learning models in forecasting water temperature.

The M5 decision tree model has proven to be a robust and versatile tool for addressing complex natural problems, demonstrating accurate results in both downscaling climate models and predicting ocean wave run-up (Yeganeh-Bakhtiary et al., 2022). Moradinejad (2024) in his research, investigated the performance of four intelligent models ANFIS, GEP, SVR and GMDH for predicting suspended sediment load at Jalayir Iran station. The findings showed that all these soft computing models have significant superiority over the classical sediment gauge curve method. Finally, the GEP model was introduced as the most efficient model with the highest coefficient of determination (0.98) and the lowest error (RMSE=3721 tons per day). Moradinejad et al. (2023) investigated computational intelligence-based modeling for estimating suspended load in the Bagharabad Qamroud River, evaluating the performance of SVM, ANFIS, and GEP models. Their results demonstrated that the GEP model outperformed the other models, with an R^2 of 0.99 and an RMSE of 0.010 tons per day. Determining the river suspended load is typically time-consuming and expensive. Thus, it is essential to select a model with high accuracy to estimate suspended sediment. However, due to variations in climatic conditions, site characteristics, and river physiography, hydrology, and hydraulic properties, a single model cannot be universally applied to all locations. Therefore, models should be calibrated and updated for each specific river. Moreover, as the river under study supplies

drinking water to Saveh City, the study and measurement of its sediment are of particular importance.

2.Material and Methods

The study area is the Pol-Doab watershed, located within coordinates 15°04'49"E to 12°52'49"E and 42°44'33" to 34°13'N, which is one of the sub-basins of Salt Lake, Iran. The watershed's outlet river is fed by three main drains including Bazneh, Shazand, and Nahrmian (Figure 1). After merging with the main tributaries of the Qarachai River, originating from Hamedan province, this river ultimately flows into the Al-Ghadir Saveh Dam. The average annual rainfall in the area is 429 mm, and the average annual temperature is 11.5 degrees Celsius.

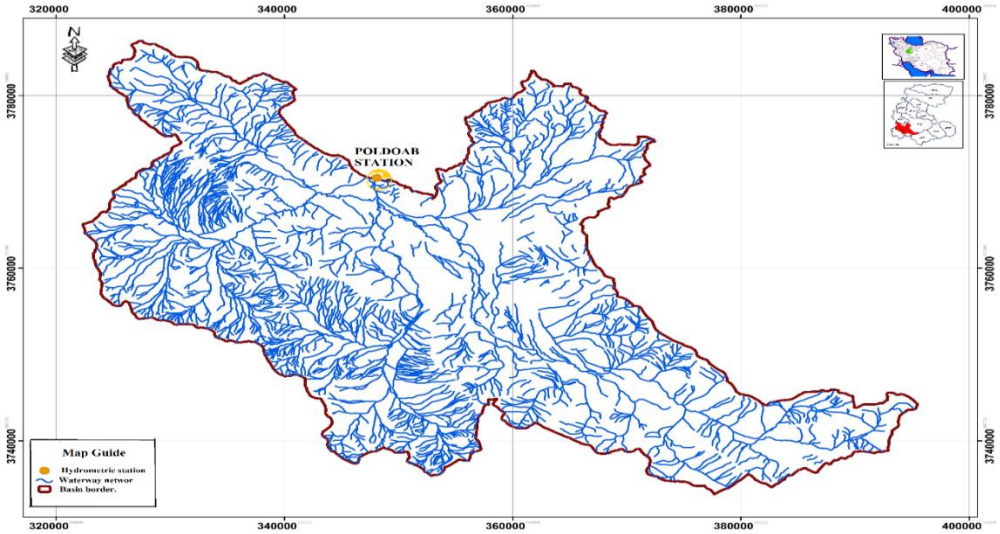

Figure 1- Location of the Study Station in the Pol Doab Area of the Qara Chai River, Markazi Province, Iran

In this study, the performance of five models was evaluated for modeling the sediment load at the Pol Doab station on the Qara Chai River in Markazi Province, Iran. The models included: Support Vector Regression (SVR), selected for its high efficiency and speed; Genetic Programming (GEP), chosen for its ability to provide explicit relationships between input and output variables; Adaptive Neuro-Fuzzy Inference System (ANFIS), due to its simplicity and high efficiency; Multivariate Adaptive Regression Splines (MARS), selected for its non-parametric regression capabilities and ability to express nonlinear and complex relationships between inputs and outputs; and the Group Method of Data Handling (GMDH), chosen for its ability to model and diagnose complex nonlinear trends, especially with limited data. It is important to note that the performance of GMDH is influenced by the characteristics of the river system, as it relies on data obtained from that system. Subsequently, the results of the five methods were compared with each other and with the results of the sediment rating curve. The most effective method was then selected. Data for this study were collected through library research, field studies, a literature review, and statistical information.

Statistics on temperature, rainfall, daily average stream discharge, and sediment load—measured daily over a 40-year period at the Pol Doab hydrometric station—were obtained from the Meteorology and Regional Water Department of Markazi Province. The collected data were categorized and converted into the required input format for the models. A sediment rating curve was developed based on discharge and corresponding sediment data, from which an equation was derived. Appropriate input variable patterns were selected through trial and error. Given the historical nature of these parameters, the design of input patterns for soft computing models incorporated time delays, similar to methods used in time series analysis and

forecasting. The model was then applied to each input-output pattern. The optimal time delay for input parameters was determined based on achieving the highest R^2 value and the lowest RMSE. In this study, 70% of the data was used for training, while 30% was allocated for validation and testing. Finally, the four data mining methods were compared with each other, along with the sediment rating curve and observational data. A summary of the range of changes and statistical characteristics of streamflow, sediment flow, precipitation, and daily temperature parameters is presented in Table 1.

Table 1- Summary Statistics of Quantitative Data at Pol Doab Station.

Variable	Observations	Minimum	Maximum	Mean	Std. deviation
P(mm)	303	0.000	83.000	2.517	8.015
T(°c)	303	-15.200	29.250	10.864	8.482
Q(m3/s)	303	0.033	110.000	6.506	15.057
S(ton/day)	303	0.000	350.330	17.979	60.351

2.1. Group Method of Data Handling (GMDH)

Ivakhnenko (1976) introduced the GMDH algorithm for identifying nonlinear relationships between input and output variables. This algorithm is a self-organizing approach applicable to modeling complex systems. The GMDH neural network comprises a multi-layer structure and a set of neurons. The connection between input and output variables can be expressed using a complex polynomial series known as the Volterra series (Equation 1).

$$\bar{y} = a_0 + \sum_{i=1}^{n} a_i X_i \sum_{i=1}^{n} \sum_{j=1}^{n} a_{ij} X_i X_j + \sum_{i=1}^{n} \sum_{j=1}^{n} \sum_{k=1}^{n} a_{ijk} X_i X_J X_K \ldots \quad (1)$$

Where X is the input variable, y is the output variable, n is the number of inputs, and a is the coefficient. The Volterra series, a general form of a mathematical equation, can be approximated using a quadratic polynomial-like equation (2). In the GMDH algorithm, all input variables are combined, and all binary combinations of these input variables are considered to generate the neurons of the first layer. For example, if m is the number of input variables, the number of neurons in the first layer is calculated as $[L1 = \binom{2}{n}]$.

$$\bar{y} = G(X_i, X_j) = a_1 X_1^2 + a_2 X_2^2 + a_3 X_1 + a_4 X_2 + a_5 X_1 X_2 + a_6 \quad (2)$$

The unknown parameters in equation (2) are polynomial coefficients determined through regression methods. These coefficients are calculated to minimize the difference between the actual output, y, and the calculated values for each pair of input variables.

2.2. Gene expression programming (GEP);

In this research, the GeneXpro Tools 4.0 model was used. GeneXproTools software, or GEP for short, is statistical software designed based on genetic programming. It is applicable to various scientific fields. Generalized genetic programming, a genetic algorithm method, was first introduced by John Koza (1992) and is based on Darwinian Theory. Gene expression programming is an automatic programming technique that solves problems using computer programs. Unlike genetic algorithms, this method does not require a predefined functional

relationship at the outset and can independently determine model components. GEP operates on tree-structured formulas rather than binary strings. These tree structures are constructed from mathematical operators (functions), problem variables, and constants (terminals) (Sultani et al., 2019).

The general form of software execution steps is shown in Figure 2. In this software environment, the following steps were followed to simulate suspended load: The first step was to select the fitting function, for which the relative root of the squared error was chosen as the fitting function for this study. The second step was input variable and function selection to generate chromosomes, which was done through a combination of flow rate, suspended sediment values, temperature, and rainfall from previous time steps. The third step involved selecting the structure and architecture of chromosomes, followed by the selection of connecting functions in the fourth step. Finally, genetic operators were selected in the fifth step. Trigonometric and exponential functions were incorporated in addition to primary conventional mathematical operators to accurately capture the mathematical relationship for estimating suspended sediments.

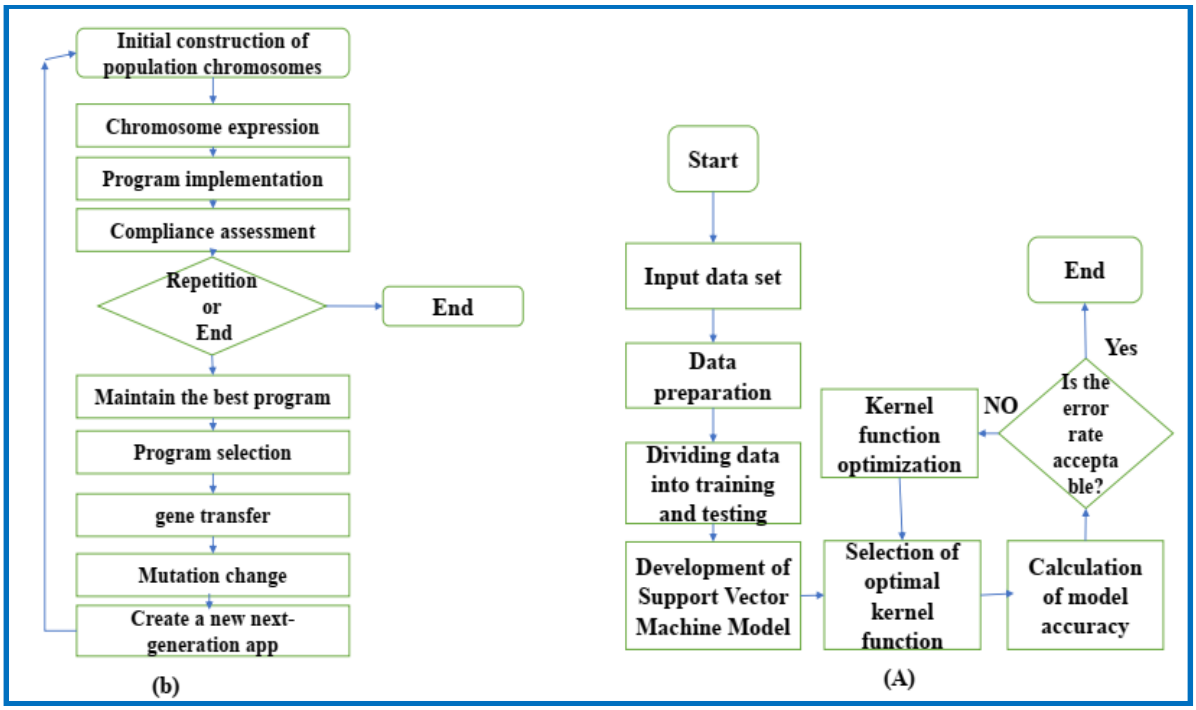

Figure 2- Implementation Steps (Flowchart): A. SVM, B. GEP

2.3. Model (MARS)

MARS is a regression algorithm introduced by Friedman in 1991 to predict continuous numerical outputs (Adamowski, 2012). This technique constructs flexible regression models by partitioning the predictor variable space into intervals and fitting spline functions (basis functions) to each interval (Zhang and Goh, 2016). A basis function represents information contained within one or more independent variables. A basis function is defined within a specific interval, with its starting and ending points referred to as nodes. Nodes are crucial to this method, as they represent points where the function's behavior changes. Essential functions, expressed by equation (3), describe the relationship between input variables and the target variable (Abraham et al., 2001).

$$hm\,(x)= \max\,(0, X-c) \quad \text{or } hm\,(x)= \max(0, c-X) \tag{3}$$

In the above relationship, c is a threshold value. Two adjacent basis functions inevitably intersect at a cross-node, ensuring the continuity of the basis functions. Basis functions are applied sequentially to each input variable, with node locations (where the function value or slope changes) determined iteratively. The number of nodes is established through trial and error. The general form of the MARS model is given by equation (4).

$$Y=f(x)=\beta_0+\sum_{m=1}^{M}\beta_m h_m(x) \quad (4)$$

In the above relationship, Y is the predicted value (target variable), determined by the function f(x). This function comprises an initial constant value, β_0, and the sum of M terms, each consisting of a coefficient, βm, and a basis function, $h_m(x)$. Initially, the MARS model estimates the objective function value with a fixed constant and then iteratively searches for the best-fitting variable-node pairs in a forward stepwise manner. This process continues until all potential basis functions are incorporated into the model, resulting in a highly complex and overfitted model with numerous nodes. In the next step, a backward pruning process is applied to the created model to identify and remove less important basis functions. This process continues until all basis functions have been evaluated. The optimal model is then selected based on minimizing the Generalized Cross Validation (GCV) criterion. Assuming GCV_K represents the GCV value for the k-th model in the elimination stage, this quantity is defined by equation (5).

$$GCV_K=\frac{\frac{1}{n}\sum_{i=1}^{n}(y_i-f_k(x_i))^2}{\left(\frac{(1-c(k))}{n}\right)^2} \quad (5)$$

In the above equation, fk represents the model estimated in the K_{th} step of the regression elimination process, and *C(k)* is derived from equation (6). In this equation, M_K equals the number of model terms in the K_{th} stage, *m* equals the number of spline function nodes in the model, and λ is a coefficient ranging from 2 to 4.

$$C_K=M_K+\lambda_m \quad (6)$$

2.4. Evaluation criteria

In order to assess the model accuracy, four statistical criteria were employed: R^2, RMSE, MBE, Nash-Sutcliffe efficiency coefficient (NS), and Taylor's diagram. R^2 determines the correlation between data and explains the variation in the range of zero to one. Higher R^2 values indicate better model performance and stronger correlations between observed and estimated data. RMSE quantifies the deviation of predicted values from observed values, with lower values signifying better model efficiency. The lower limit of RMSE is zero. A lower MBE indicates a more influential model. The Nash-Sutcliffe efficiency (NS) coefficient ranges from zero to one, with values closer to one signifying higher model efficiency in forecasting. A perfect fit is indicated by NS equal to one. Simulation results are considered excellent for NS values above 0.75 and satisfactory between 0.36 and 0.75. Equations (7) to (10) provide the calculation methods for these statistical indicators.

$$R^2=\frac{\sum_{i=1}^{n}(x_o-\overline{x_o})(x_c-\bar{x}_c)}{\left(\sum_{i=1}^{n}(x_o-\overline{x_o})^2\right)^{0.5}\left(\sum_{i=1}^{n}(x_c-\overline{x_c})^2\right)^{0.5}} \quad (7)$$

$$RMSE=\sqrt{\frac{\sum_{i=1}^{n}(x_o-x_c)^2}{n}} \quad (8)$$

$$NS=1-\frac{\sum_{i=1}^{n}(X_O-X_C)^2}{\sum_{i=1}^{n}(X_O-\bar{X}_O)^2} \quad (9)$$

$$MBE=\frac{1}{n}\sum_{i=1}^{n}(x_o-x_c) \quad (10)$$

3.Results and Discussion

Normality tests were conducted using XLSTAT statistical software, and the results are summarized in Table 2. The Shapiro-Wilk, Anderson-Darling, Lilliefors, and Jarque-Bera tests were employed to assess whether the data followed a normal distribution. In all cases, the null hypothesis assumed normal distribution, while the alternative hypothesis indicated non-normality. The results of all tests confirmed that the data were not normally distributed. Specifically, the temperature, rainfall, streamflow, and sediment load data at the Pol Doab station showed significant deviations from normality. Table 3 presents the results of the correlation analysis. A strong and statistically significant positive relationship was observed between suspended sediment load and stream discharge (r=0.808, r = 0.808, r=0.808) and between suspended sediment load and rainfall (r=0.077, r = 0.077, r=0.077) at the 99% confidence level. Additionally, a significant negative correlation was identified between precipitation and temperature (r=−0.020, r = -0.020, r=−0.020) at the same confidence level. These findings suggest that increases or decreases in river discharge and rainfall are associated with corresponding changes in suspended sediment load.

In contrast, the inverse relationship between temperature and precipitation indicates that an increase in temperature corresponds to a decrease in precipitation, and vice versa. Further analysis revealed a significant positive relationship between discharge and rainfall at the 99% confidence level. Among all the variables, sediment load exhibited the greatest deviation from normality, followed by streamflow. Normal probability quantile–quantile (Q-Q) plots were also used to visually assess the extent of deviation from normality. These plots provided insight into the potential impacts of non-normality on regression model performance. To ensure the reliability of the dataset, a standard normal homogeneity test was conducted—an established method for evaluating data consistency over time. Figures 4 and 5 display the correlation map and matrix, respectively, illustrating the interrelationships among the variables. Figures 3 to 8 present the frequency distributions for precipitation, temperature, sediment load, and daily river discharge. These figures clearly show that none of these variables follow a normal distribution at the Pol Doab station on the Qara Chai River.

It is important to note that data mining methods do not require the input variables to follow a normal distribution. This is a key advantage over traditional statistical techniques, which often rely on the assumption of normality for accurate results. Unlike these conventional methods, data mining models are free from distributional assumptions, making them well-suited for analyzing complex and non-normally distributed environmental data (Mehrizi Haeri, 2012; Sattari et al., 2015).

Table 2- Results of Normality Tests for Data at Pol Doab Station.

Test	Shapiro-Wilk test			Anderson-Darling test			Lillie-Force test			Jarko Bra test		
parameter	P-value	Probability of rejecting	Confidence level α	P-value	Probability of rejecting	Confidence level α	P-value	Probability of rejecting	Confidence level α	P-value	Probability of rejecting	Confidence level α
P	<0.0001	0.01	0.05	0.0001	0.01	0.05	0.0001	0.01	0.05	0.0001	0.01	0.05
T	<0.0001	0.01	0.05	0.0001	0.01	0.05	0.0001	0.01	0.05	0.0001	0.01	0.05
Q	<0.0001	0.01	0.05	0.0001	0.01	0.05	0.0001	0.01	0.05	0.0001	0.01	0.05
S	<0.0001	0.01	0.05	0.0001	0.01	0.05	0.0001	0.01	0.05	0.0001	0.01	0.05

Table 3- Pearson correlation matrix at Pol Doab station (α <0.01).

Variables	S(ton/day)	Q(m3/s)	P(mm)	T
S(ton/day)	**1**	**0.808****	0.077	-0.020
Q(m3/s)	**0.808**	**1**	**0.208**	**-0.116**
P(mm)	0.077**	**0.208**	**1**	**-0.209**
T(°C)	-0.020**	**-0.116**	**-0.209**	**1**

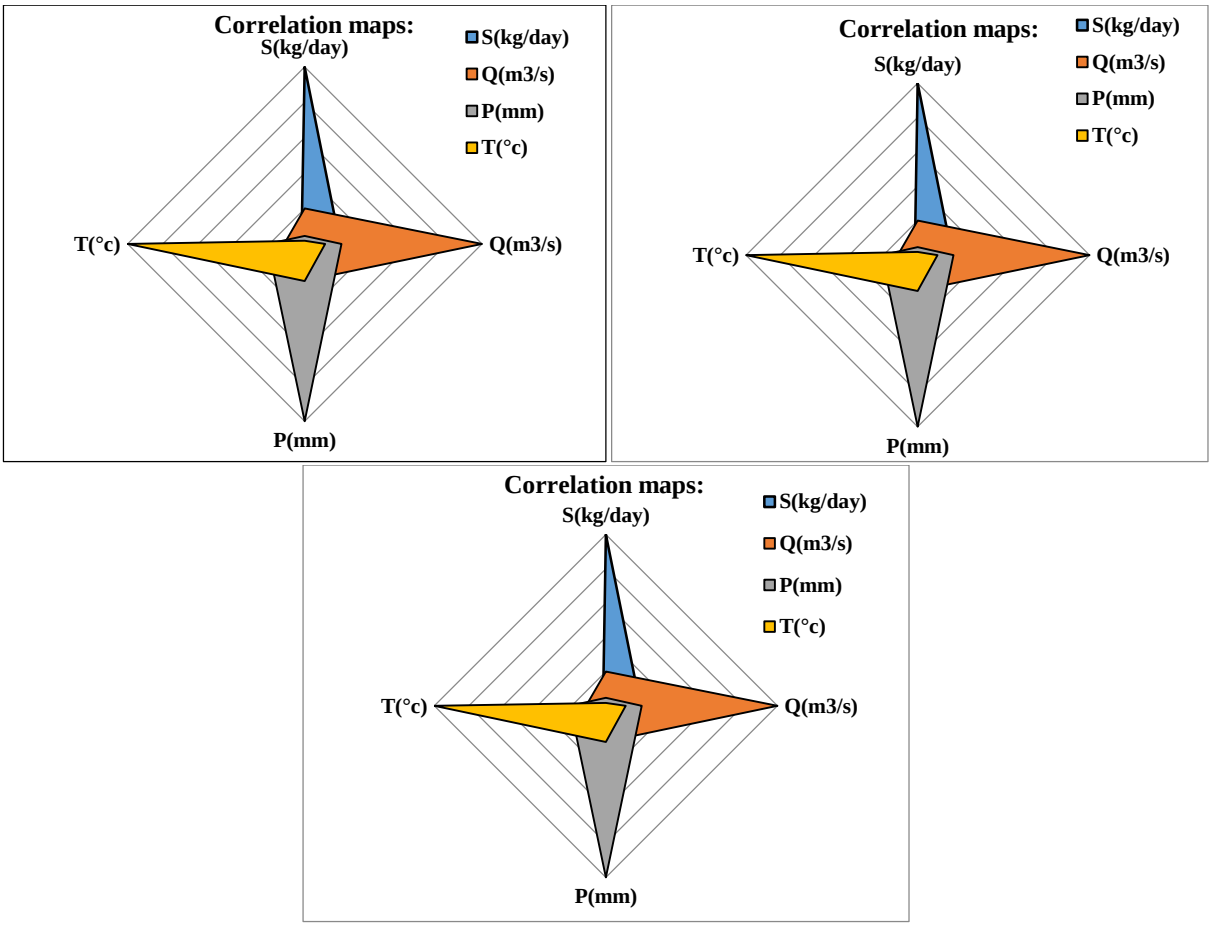

Figure 3- Correlation maps between parameters at Pol Doab station.

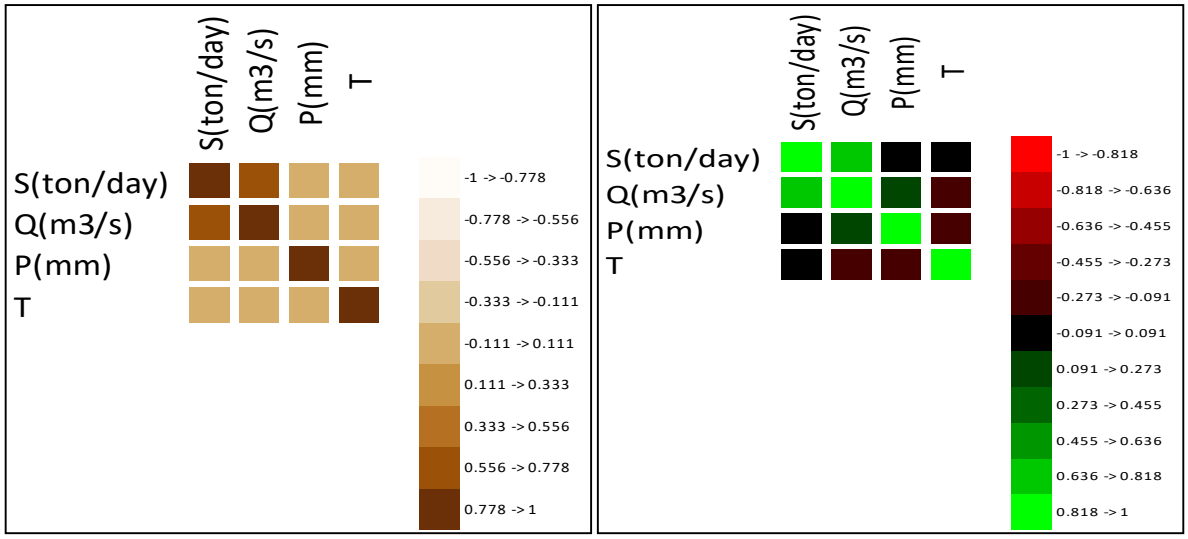

Figure 4- Correlation matrix image at Pol Doab station.

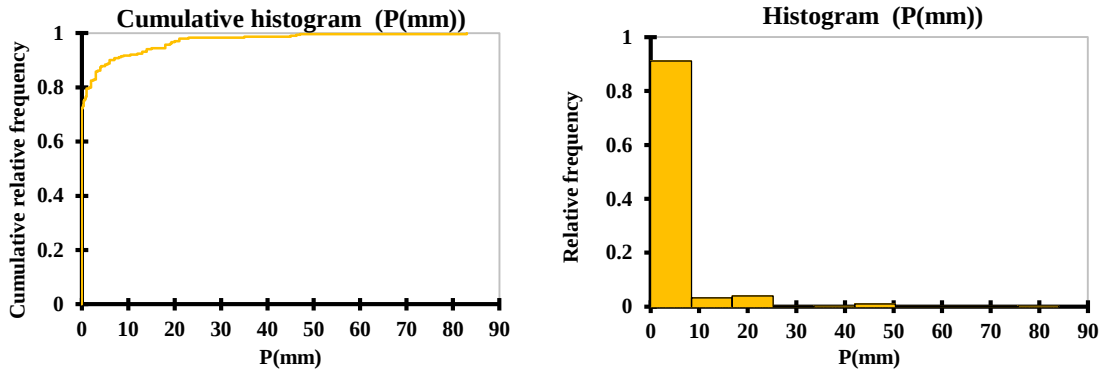

Figure 5-Histogram and frequency of daily rainfall data at Pol Doab station.

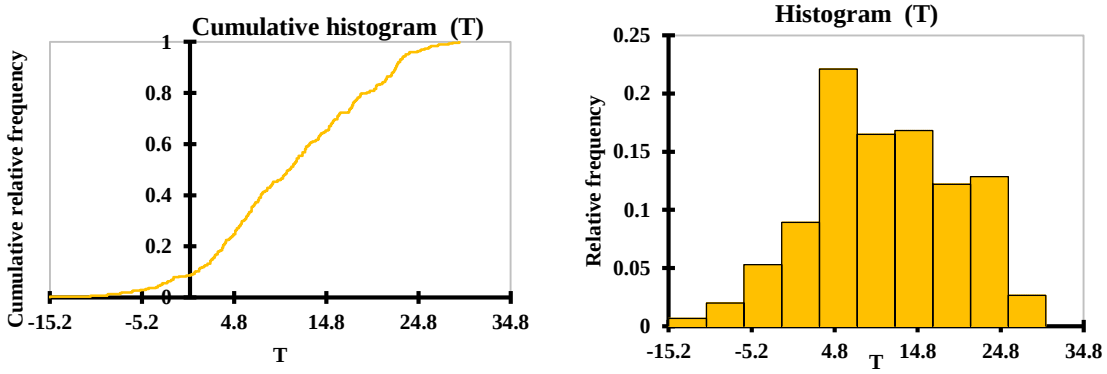

Figure 6- Histogram and frequency of daily temperature data at Pol Doab station.

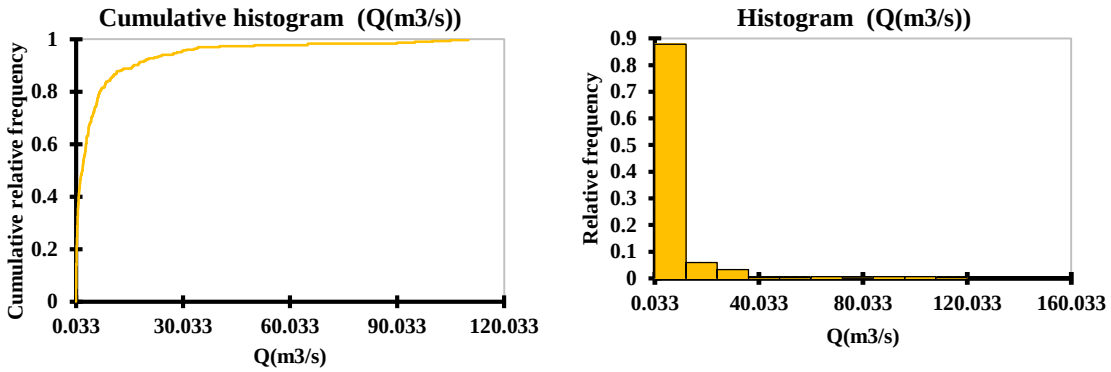

Figure 7- Histogram and frequency of daily flow discharge data at Pol Doab station.

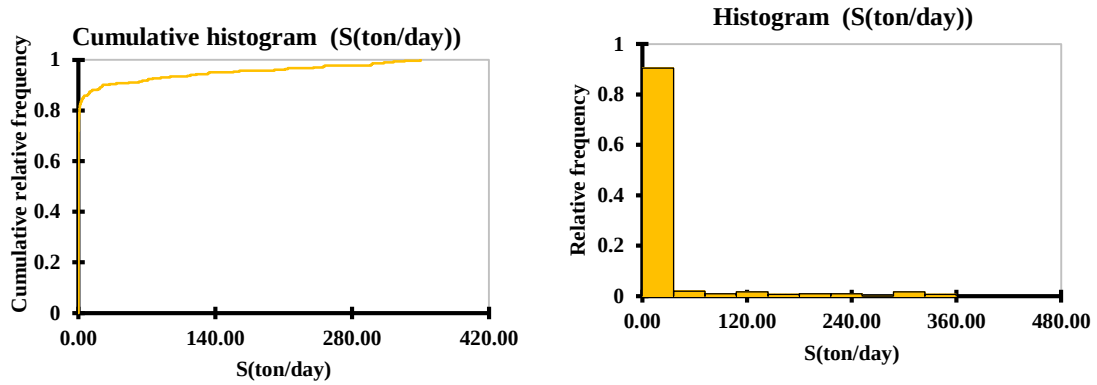

Figure 8- Histogram and frequency of daily sediment data at Pol Doab station.

Sediment rating curves were developed based on river measurements. For each specific river discharge, the corresponding concentration of suspended sediment was measured, and a curve was plotted. Figure 10-a displays the sediment rating curve for the training phase at Pol Doab station. A P-P plot was constructed in Figure 9-b to assess data normality. This plot compares the cumulative probability of observed data to the cumulative probability of values calculated from the obtained equation. The data was initially divided into 70% for training and 30% for testing.

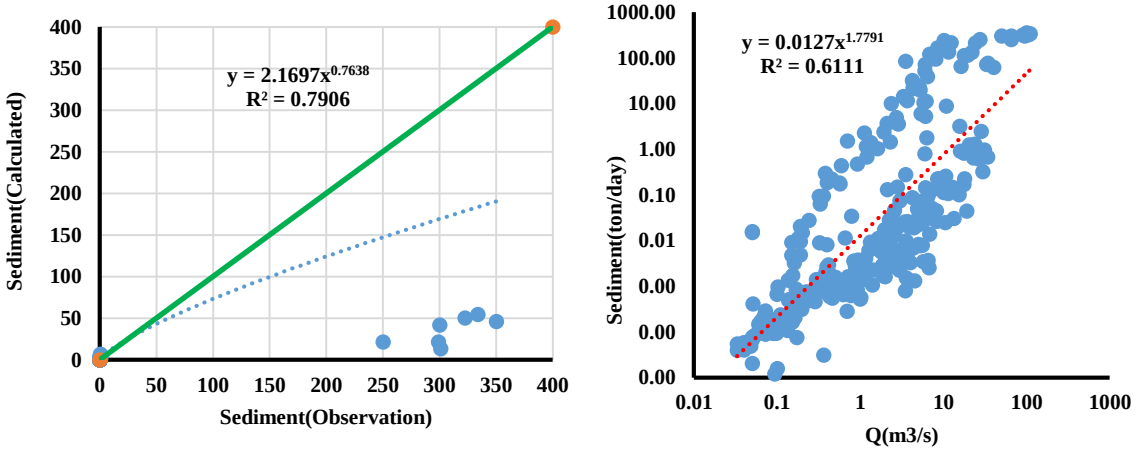

Figure 9- A. Sediment measurement curve of the training part, B. Calculation and observation values for the test part

In order to estimate suspended sediment, various input patterns were utilized, such as temperature, rainfall, sediment, and flow rate from both current and previous time steps. This approach aimed to determine the impact of each variable on suspended sediment modeling.
Among the investigated models, SVR was initially selected due to its superior efficiency and speed in the modeling process. The model was implemented using a program developed in the MATLAB software environment. In the first step, 13 different scenarios (f1 to f13), as outlined in Table 4, were employed as input patterns for the SVR model. Scenario selection was based on a combination of literature review, expert knowledge, trial and error, weather conditions, the mountainous terrain, and river characteristics.

Table 4- Different scenarios are used for the models

Function	Number	Function	Number
Q_t, Q_{t-1}, S_t	(f8)	Q_t, S_t, T_t, P_t	(f1)
Q_t, Q_{t-2}, Q_{t-1}, S_{t-1}, S_t	(f9)	Q_t, Q_{t-1}, S_{t-1}, S_t, T_t, P_t, P_{t-1}	(f2)
Q_t, Q_{t-1}, S_{t-1}, S_t, P_t	(f10)	Q_t, S_{t-1}, S_t	(f3)
Q_t, Q_{t-1}, S_{t-1}, S_t, T_t, T_{t-1}	(f11)	Q_t, S_t, T_t	(f4)
Q_t, Q_{t-1}, S_{t-1}, S_t, T_t, T_{t-1}, P_{t-1}, P_t	(f12)	Q_t, S_t, P_t	(f5)
Q_t, Q_{t-1}, S_{t-1}, S_t, P_{t-1}, P_t	(f13)	Q_t, Q_{t-1}, S_{t-1}, S_t	(f6)
		Q_t, S_t	(f7)

At the Pol Doab station, data were organized, and the independent and dependent variables were identified for each input pattern or scenario. These data were then used as inputs for the Support Vector Regression (SVR) model, which was executed accordingly. Each model was run 15 times, and the average values of the coefficient of determination (R^2) and root mean square error (RMSE) from these iterations were calculated and are presented in Table 5. This table summarizes the performance of the SVR model across 13 different input patterns, including statistical error indices and optimal parameter values (σ) for each model. By comparing the 13 models, the one with the highest R^2 and lowest RMSE was selected as the best-performing model. According to Table 5 and the statistical error indices, the highest performance was observed for model number 6. This model used the flow rate on the same day, along with flow rate and suspended sediment data from the previous time step, as inputs. In contrast, the poorest performance was associated with model number 7, which utilized only the flow rate from the same day. This outcome suggests that suspended sediment concentrations are highly dependent on both the flow rate and sediment data from the previous time step. For the best-performing model (model 6), the R^2 and RMSE values were 0.98 and 185 tons/day, respectively, during the test phase, and 0.83 and 248 tons/day during the training phase. These findings are consistent with those reported by Aytek and Kisi (2008). Moreover, comparisons with the studies by Kisi et al. (2012) and Sattari et al. (2015) further support the current results. Their research indicated that optimal input combinations for intelligent models included suspended sediment from the previous time step and flow rate data from both the current and previous time steps, corroborating the findings of the present study. Additionally, Table 5 shows that models 1 and 2 yielded reasonably satisfactory results. Model 3, which used the current day's flow rate and the previous time step's suspended sediment concentration, also produced relatively acceptable statistical indicators, confirming a strong correlation between suspended sediment and the current flow rate. However, the inclusion of current flow rate and temperature (model 4), as well as current flow rate and rainfall (model 5), resulted in comparatively weaker model performance. In contrast, the use of delayed flow and sediment data (model 6) enhanced

model performance significantly. Models using only the current day's flow rate (model 7) demonstrated poor predictive accuracy. Models 8 through 13 showed varying degrees of improvement. Figures 10 to 12 illustrate the SVR model outputs for the best-performing input pattern (model 6), including time series plots and scatter plots of observed versus simulated suspended sediment values. These figures demonstrate that the SVR model effectively captured the nonlinear and complex relationships between the input and output variables. Overall, the findings in this section suggest that excluding temperature and rainfall variables improved the model's predictive performance significantly.

Table 5- Parameter values and performance metrics of the SVR model for various input patterns during the test period at Pol Doab station.

Statistical indicators of performance in the test phase.			Statistical indicators of performance in the training phase			Model
R^2	σ	RMSE (ton/day)	R^2	σ	RMSE (ton/day)	
0.81	24	24	0.62	38.8	38.7	**SVR1**
0.85	315	314	0.99	6.65	6.63	**SVR2**
0.95	640	641	0.46	455.7	454.6	**SVR3**
0.32	243	263	0.34	13665.4	664.2	**SVR4**
0.48	144	152	0.35	670.44	668.8	**SVR5**
0.98	186	185	0.83	249.4	248.8	**SVR6**
0.31	721	719	0.28	554.7	553	**SVR7**
0.65	509	506	0.94	137	137	**SVR8**
0.94	575	574	0.90	192	191	**SVR9**
0.86	207	209	0.99	13	13	**SVR10**
0.76	300	305	0.99	20	20	**SVR11**
0.92	368	470	0.99	3.76	3.75	**SVR12**
0.79	185	185	0.99	7.13	7.11	**SVR13**

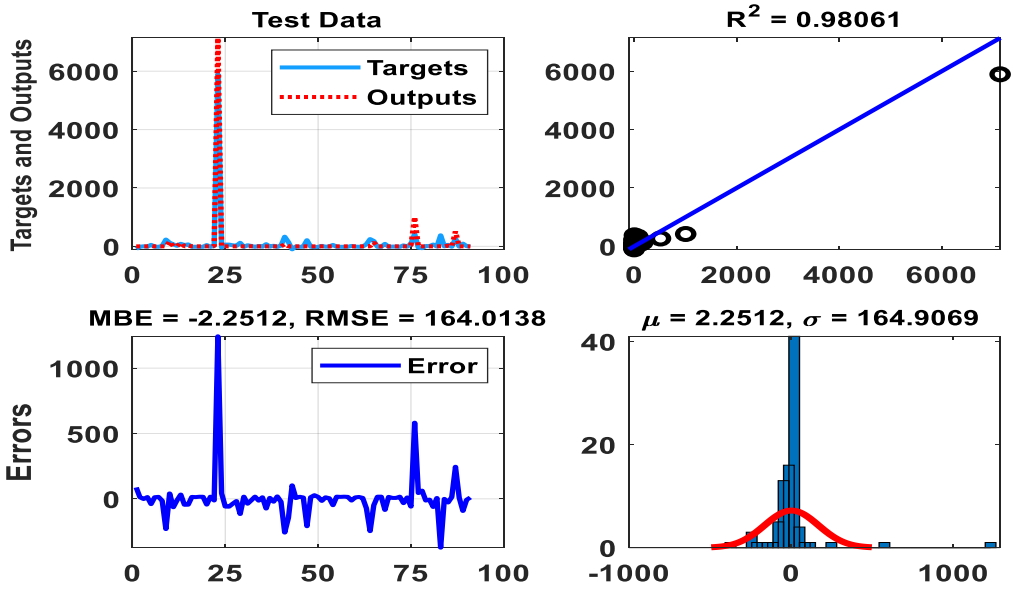

Figure 10- The output results of the SVR model in the MATLAB environment at the test stage of the Pol Doab station.

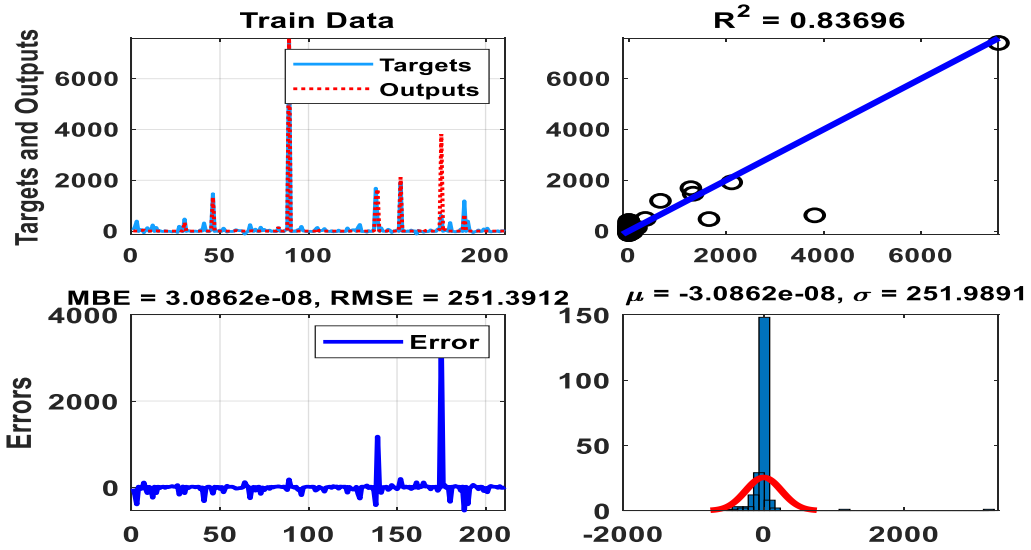

Figure 11-The output results of the SVR model in the MATLAB environment during the training phase of the Pol Doab station.

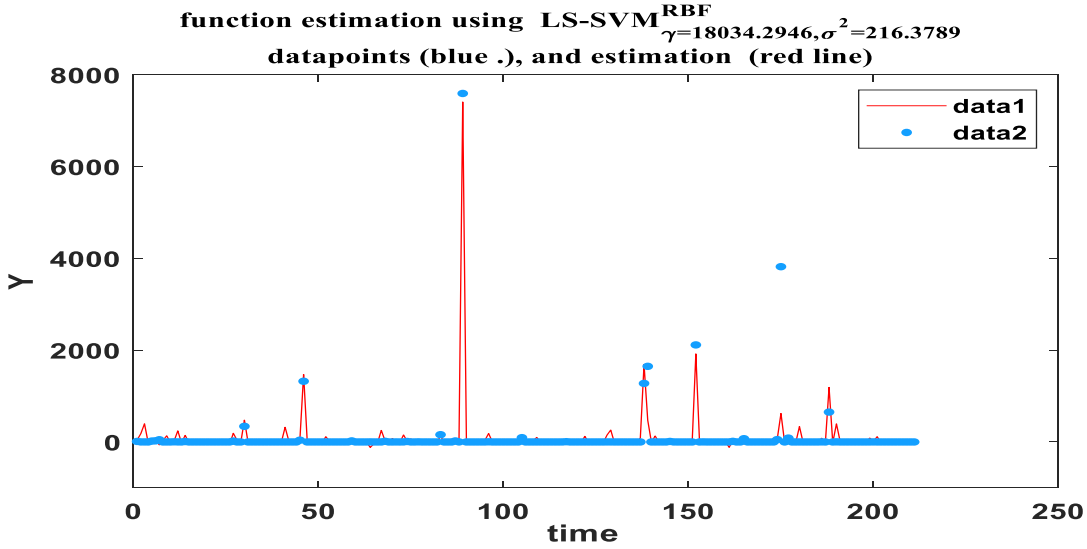

Figure 12- Output results of SVR model and actual data at the Pol Doab station.

3.1. Results of the ANFIS Method at the Pol Doab Station

Following data preprocessing at the Pol Doab station, including sorting and identifying the independent and dependent variables for each model or scenario, the dataset was input into the Adaptive Neuro-Fuzzy Inference System (ANFIS) model and executed. Each model was run 15 times, and the average coefficient of determination (R^2) and root mean square error (RMSE) values from these runs were calculated. The results are presented in Table 6, which summarizes the performance of the ANFIS model across 13 different input patterns. The table includes statistical error indices and the corresponding optimal parameter values (σ) for each model. Subsequently, the outputs of the 13 models (scenarios) were compared, and the model with the

highest R^2 and lowest RMSE was selected as the best-performing model. Based on these criteria, model number 1 was identified as the most accurate, demonstrating the highest explanatory power (R^2) and the lowest prediction error (RMSE). Different data partitioning strategies were evaluated to optimize the ANFIS model's performance. One commonly used approach is network partitioning, which involves selecting the type and number of membership functions (MFs) for each input variable. Common MF types include triangular, trapezoidal, Gaussian, and bell-shaped functions. In this study, several membership function types were assessed using the optimal input configuration (model no. 1), and their corresponding RMSE values were reported in Table 7. The triangular membership function yielded the lowest RMSE, indicating superior performance. According to Table 7, the optimal configuration involved using two, two, and four membership functions for flow rate, volume, and temperature (at the current time step). These findings are consistent with those reported by Russell and Campbell (1996), who also found that triangular membership functions tend to deliver better practical results.

Table 6- Parameter values and performance metrics of the ANFIS model for various input patterns during the test period.

Statistical indicators of performance in the test phase.			Statistical indicators of performance in the training phase			Model
R^2	σ	RMSE (ton/day)	R^2	σ	RMSE (ton/day)	
0.79	24	24	0.70	34	34	F1
0.51	356	275	0.33	630	629	F2
0. 95	718	717	0.81	256	255	F3
0.25	786	282	0.70	584	583	F4
0.36	833	837	0.76	549	547	F5
0.86	711	720	0.89	253	253	F6
0.35	880	880	0.11	517	516	F7
0.51	1068	1072	0.33	324	323	F8
0.85	405	404	0.83	244	244	F9
0.57	121	136	0.31	664	663	F10
0.53	250	256	0.31	654	652	F11
0.78	36598	36612	0.94	223	223	F12
0.24	235	251	0.35	645	643	F13

Table 7-The performance of the ANFIS model according to different membership functions for the optimal model.

RMSE (ton/day)	Number of membership functions	Membership function type
24	2,2,4	Triangular
261	2,3,4	Gossi
284	2,2,3	trapezoidal
345	3,2,2	a bell

3.2. Results of the GEP Method at the Pol Doab Station

The results of the Gene Expression Programming (GEP) method at the Pol Doab station are presented in this section. GEP is an evolutionary algorithm inspired by Darwinian principles of natural selection. A distinguishing feature of the GEP model, compared to other soft computing techniques, is its ability to generate an explicit algebraic expression for estimating the target

variable (Ferreira, 2001). In this study, the GEP model was implemented using GeneXpro Tools 4.0 software. The simulation of suspended sediment load involved the following steps:

1. Selection of the Fitness Function: The relative root squared error (RRSE) was chosen as the fitness function to evaluate model performance.
2. Selection of Input Variables and Functions: A combination of flow rate, suspended sediment concentration, temperature, and rainfall—drawn from both the current and previous time steps—was considered as input data. These variables were used to generate chromosomes.
3. Definition of Chromosome Structure: The architecture of the chromosomes was defined, including the number of genes and the linking function used to combine them.
4. Specification of Linking Functions: Appropriate linking functions were selected to determine how genes interact within the chromosome.
5. Selection of Genetic Operators: Genetic operators, including mutation, crossover, and transposition, were selected. In addition to basic arithmetic operators, trigonometric and exponential functions were also included to enhance the model's ability to express complex mathematical relationships.

A key advantage of the GEP model over other intelligent algorithms is its ability to provide interpretable mathematical equations describing the relationship between input and output variables, which is particularly valuable for forecasting applications. Following a sensitivity analysis of the GEP model's performance in estimating suspended sediment load, the parameters and genetic operators used—along with their corresponding values—are summarized in Table 8.

Table 8- ***Parameter values and genetic operators used in the GEP model at the Pol Doab station.***

Genetic operators		General settings	
0.044	Mutation rate	30	Number of chromosomes
0.1	Inversion rate	7	head size
0.1	Consecutive insertion tranche rate	3	Number of genes per
0.1	The rate of his song is the root of	100000	Number of production
0.3	Single point combination rate	Sum (+)	Link function

As entioned previously, the first step in using the GEP model is to select the appropriate fitting function. In this study, results indicated that the RRSE fitting function outperformed other options for suspended sediment modeling. Therefore, the RRSE function was chosen as the fitting function for the model. The next step involved selecting the main operators to build the parse tree. The mathematical functions used in this research and the model's performance for specific function sets are presented in Table 9. In this table, the performance of the GEP model for 13 different input patterns is shown in terms of statistical error indicators and the optimal parameter values for each model. The 13 models (scenarios) were compared, and the one with the highest R^2 and lowest RMSE was selected. According to Table 9 and the statistical error indicators, the GEP3 model achieved the best performance for model number 3. Table 9 also indicates that the lowest RMSE value was obtained for the GEP3 function.

Table 9- Values of parameters and performance of the GEP model for different input patterns in the training and test period.

Statistical indicators of performance in the test phase.					Statistical indicators of performance in the training phase					Model
RRSE	MAE	MSE	RMSE (ton/day)	R^2	RRSE	MAE	MSE	RMSE (ton/day)	R^2	
0.772	4.92	40.84	6.39	0.41	0.864	6.00	53.60	7.32	0.25	SVR1
0.654	4.23	29.83	5.46	0.57	0.816	5.66	47.95	6.92	0.35	SVR2
0.137	0.240	0.55	0.745	0.98	0.229	41.34	0.00023	152	0.95	SVR3
0.813	5.42	45.64	6.75	0.34	0.892	6.30	57.22	7.56	0.31	SVR4
0.277	0.831	2.25	1.50	0.93	0.451	90.94	0.00090	299.77	0.79	SVR5
0.165	0.498	0.80	0.894	0.97	0.225	35.04	0.00022	149.5	0.95	SVR6
0.17	0.45	0.84	0.915	0.97	0.553	130	0.000013	367	0.70	SVR7
0.289	0.707	2.45	1.56	0.92	0.379	76.42	0.00063	251.5	0.86	SVR8
0.363	0.89	3.90	1.98	0.87	0.208	33.77	0.00019	138	0.95	SVR9
0.064	3.22	27.43	5.24	0.99	0.360	10	473	22	0.87	SVR10
0.487	3.26	16.70	4.08	0.76	0.604	3.90	26.3	5.12	0.64	SVR11
0.470	2.87	15.60	3.95	0.78	0.571	6.70	23.5	4.85	0.67	SVR12
0.085	3.16	48.38	6.95	0.99	0.425	13.01	660	25.70	0.82	SVR13

The next step involved selecting the primary mathematical operators for constructing the parse tree. The mathematical functions applied in this study, along with the model's performance using specific function sets, are presented in Table 10. This table summarizes the impact of various mathematical function combinations on the R^2, RMSE, and MAE indices at the Pol Doab station. According to the results in Table 10, function set *f5* produced the best performance in terms of predictive accuracy. Once the optimal combination of mathematical functions was identified, the next step was to determine the most suitable linking function. Among the tested options—addition, subtraction, multiplication, and division—the multiplication linking function outperformed the others, as confirmed by the results shown in Table 10. Figure 13 illustrates the parse tree generated for estimating suspended sediment using input pattern No. 3. This figure highlights the strong influence of suspended sediment values from the previous time step and current discharge levels on sediment prediction, supporting the conclusions drawn in earlier sections. Figure 14 displays the time series and scatter plots of observed versus simulated suspended sediment values during the test period using the GEP model. The results indicate that the GEP model provides accurate and meaningful predictions, effectively capturing both the general trends and peak values of suspended sediment.

Table 10- ***Effect of different mathematical function sets on the RMSE, MAE, and R^2 values in the GEP model at the Pol Doab station.***

R^2	MAE	RMSE (ton/day)	Mathematical model	Function
0.98	0.259	0.760	+ - * /	F1
0.95	0.604	1.25	+ - * / lnx, e^x	F2
0.93	0.590	1.38	+ - * /, $\sqrt{X}$, $\sqrt[3]{X}$, x^3, x^2	F3
0.95	0.609	1.25	+ - * / lnx, e^x, $\sqrt{X}$, $\sqrt[3]{X}$, x^3, x^2	F4
0.98	0.224	0.634	+ - * / lnx, e^x, $\sqrt{X}$, $\sqrt[3]{X}$, x^3, x^2, sinx, cosx, Arctg x	F5
				Link function type
-	1.61	5.38	+	plural
-	1.61	5.38	-	subtraction
0.84	0.500	2.11	×	multiplication
0.80	0.596	2.38	/	**Division**

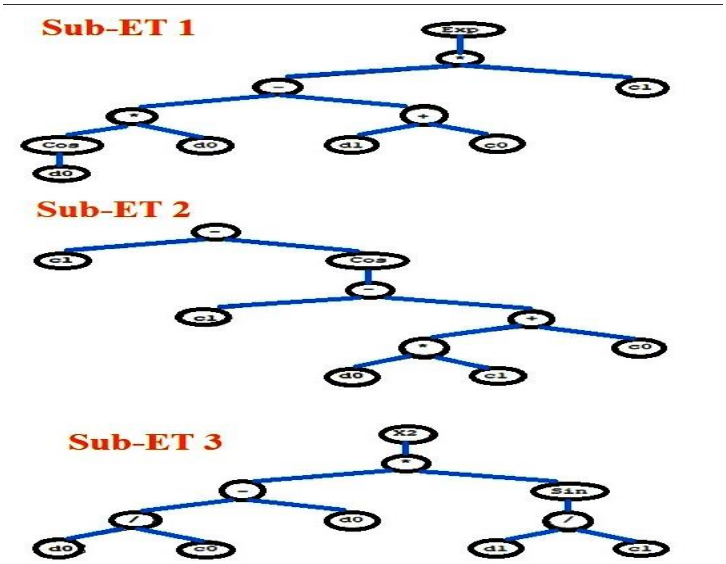

Figure 13- Tree diagram for suspended sediment estimation based on input pattern No. 3 at the Pol Doab station.

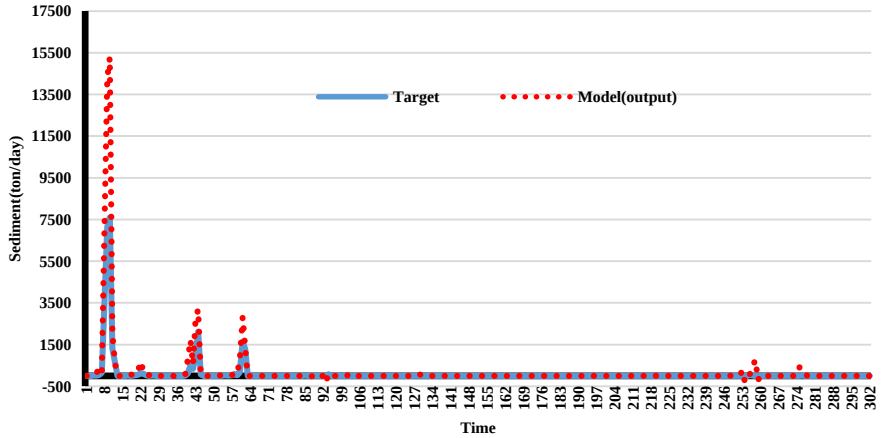

Figure 14- Time series graph of observed and calculated sediment values from the model at the Pol Doab station.

The following presents the results of modeling and estimating the suspended sediment load using the MARS model. Table 11 details the essential functions and coefficients of the MARS model, which was developed based on scenario f3 in equation (11). In the initial modeling stage, 45 essential functions were considered. This number was reduced to 15 essential functions through pruning, ultimately resulting in an optimal multivariate adaptive regression model composed of 30 main functions. The optimal models derived from the multivariate adaptive regression model are presented in equation (11). Additionally, Table 11 outlines the essential functions derived from the multivariate adaptive regression model for the station used in this research. By partitioning the problem space into intervals of predictor variables (inputs) and fitting a spline (basis function) within each interval, the MARS model creates flexible regression models for predicting the target variable. The importance of each input parameter can be determined based on the number of repetitions and the coefficient associated with it within the MARS model (Zhang and Goh, 2016). Table 12 presents the error statistics of the MARS model developed based on the f3 scenario.

$$S_t = 0.541 + \sum_{i=1}^{30} C_i * BF_i \qquad (11)$$

Table 11-Basis functions and their coefficients in the MARS model to estimate the suspended sediment load at Pol Doab station.

Row	Basis functions	coefficients
1	BF1 = max(0, S(t-1) -0.0677)	0.541
2	BF2 = max(0, 0.0677 -S(t-1))	12.244
3	BF3 = BF1 * max(0, Q(t-1)-0.300)	-12.176
4	BF4 = BF1 * max(0, 0.300 -Q(t-1))	-471.539
5	BF5 = max(0, 0.3089-Q(t)) * max(0, S(t-1) -0.0677)	-26.870
6	BF6 = BF2 * max(0, Q(t) -0.0871)	15.467
7	BF7 = max(0, 0.248-Q(t)) * max(0, S(t-1) -0.0001)	23.576
8	BF8 = max(0, 0.248-Q(t)) * max(0, 0.0001 -S(t-1))	122.803
9	BF9 = max(0, 0.3089-Q(t)) * max(0, S(t-1) -0.0001)	14936.217
10	BF10 = max(0, 0.3089-Q(t)) * max(0, 0.0001 -S(t-1))	-118.834
11	BF11 = max(0, 0.011-S(t-1))	-11727.430
12	BF12 = BF11 * max(0, Q(t) -0.0736)	5.486
13	BF13 = BF11 * max(0, 0.0736 -Q(t))	-199.677
14	BF14 = max(0, 0.248-Q(t)) * max(0, 0.0548-Q(t-1))	-143.960
15	BF15 = BF2 * max(0, Q(t) -0.0736)	21.667
16	BF16 = BF11 * max(0, Q(t-1)-0.010)	41.603
17	BF17 = max(0, 0.3089-Q(t)) * max(0, Q(t-1)-0.177)	-3.936
18	BF18 = max(0, 0.3089-Q(t)) * max(0, 0.177 -Q(t-1))	-37.707
19	BF19 = max(0, S(t-1) -0.011) * max(0, Q(t-1)-0.146)	50.301
20	BF20 = max(0, 0.248-Q(t)) * max(0, Q(t-1)-0.010)	-32.685
21	BF21 = max(0, 0.248-Q(t)) * max(0, 0.010 -Q(t-1))	-13.165
22	BF22 = max(0, Q(t) -0.185)	15.126
23	BF23 = max(0, 0.185 -Q(t))	-2.189
24	BF24 = BF23 * max(0, Q(t-1)-0.219)	1.714
25	BF25 = BF23 * max(0, 0.0548-Q(t-1))	-21.979
26	BF26 = max(0, 0.3089-Q(t)) * max(0, Q(t-1)-0.146)	-29.805
27	BF27 = max(0, 0.3089-Q(t)) * max(0, 0.146 -Q(t-1))	28.295
28	BF28 = max(0, 0.248-Q(t)) * max(0, Q(t-1)-0.146)	-48.846
29	BF29 = max(0, 0.248-Q(t)) * max(0, 0.146 -Q(t-1))	34.711
30	BF30 = BF23 * max(0, S(t-1) -2.225e-05)	-15.563

Table 12- Statistical characteristics of the accuracy of the MARS model.

Train							Test						
R^2	RMSE	MAD	MBE	MSE	NS	MAPE	R^2	RMSE	MAD	MBE	MSE	NS	MAPE
0.99	0.005	0.003	-0.0019	0.000	0.99	606820	0.93	0.026	0.009	-0.008	0.001	0.75	820667

3.3. Application of Optimal Input Patterns from SVM, ANFIS, MARS, and GEP in the GMDH Model

In the next phase of analysis, the best-performing input patterns identified from the SVM, ANFIS, MARS, and GEP models were used as inputs for the Group Method of Data Handling (GMDH) model. Specifically, input pattern 6, which was selected as the optimal configuration for the SVM model, was introduced into the GMDH model. During the training and testing phases, the model yielded R^2 values of 0.99 and 0.79, respectively. The corresponding RMSE values were 83 and 221 tons/day, MSE values were 6,937 and 48,918, and standard deviation (StD) values matched the RMSE values. In addition, the optimal input patterns from the ANFIS (pattern 1) and GEP (pattern 3) models were also introduced into the GMDH model for comparative analysis. The performance results of the GMDH model are presented in Table 13. Figures 15 and 16 illustrate the GMDH model's output during the training and testing phases at the Pol Doab station. The high R^2 (0.99) and low RMSE (83 tons/day) during training indicate a strong model fit and predictive capability. Figure 17 provides a visual comparison between observed and modeled suspended sediment data using the GMDH model, revealing that the model effectively captured both the general trends and the peak sediment values. Furthermore, Table 13 and Figure 18 (Taylor diagram) summarize the statistical performance indicators of the GEP, ANFIS, SVR, MARS, GMDH, and SRC (Sediment Rating Curve) models using their respective optimal input patterns. The results show that the GEP model outperformed all other models, including the traditional sediment rating curve. The GMDH, ANFIS, SVR, and MARS models ranked second through fifth, respectively. All four data mining models demonstrated significantly better performance than the SRC model. The GEP model, in particular, proved to be a powerful tool for modeling suspended sediment in the Pol Doab catchment. It exhibited strong performance in predicting peak sediment loads, which are essential for estimating reservoir storage capacity and the hydraulic design of infrastructure. Compared to the SRC method, machine learning approaches demonstrated superior precision and accuracy. This advantage is attributed to the inherent limitations of the SRC method, which relies heavily on regression relationships predominantly formed from low-flow data. As most sediment transport occurs during high-flow events, the SRC method often fails to accurately capture sediment peaks. Additionally, converting results from logarithmic to arithmetic space in the SRC method can lead to an underestimation of sediment loads. Intelligent models such as GEP, ANFIS, SVR, MARS, and GMDH offer accurate estimates of suspended sediment load (SSL), even when data quantity and quality are limited. The superior performance of certain models can be attributed to specific strengths. For example, the SVM model demonstrates high accuracy and efficiency due to its capacity to determine optimal decision boundaries in the feature space. In contrast, artificial neural networks may terminate the learning process prematurely upon reaching a local minimum, potentially resulting in suboptimal performance.

Execution time is another consideration: SVM models generally require less computational time, as they are less sensitive to the number of data categories. Neural networks, by contrast, have execution times influenced by factors such as the number of training samples, the number of neurons in hidden layers, learning functions, learning rates, and momentum values—many of which must be tuned through trial and error. Regarding execution speed, the SRC model is the fastest, followed by ANFIS, SVM, and GEP. A notable advantage of the GEP model is its ability to produce a mathematical expression representing the relationship between input and output variables, making it valuable for future forecasting and analysis. This feature may make it preferable to the other three models, despite the complexity of the relationships it generates.

Future studies could further explore the effects of different input parameters on sediment transport processes and improve model performance by employing parameter optimization techniques, such as derivative-based algorithms or evolutionary methods like genetic algorithms.

Table 13-*Comparison of model performance in estimating suspended sediment load using the best input pattern at the Pol Doab station.*

NS	MBE	RMSE (ton/day)	R2	Optimal Pattern	Model
0.89	-5.42	185	0.98	F6	**SVR**
0.85	1.90	24.3	0.79	F1	**ANFIS**
0.98	0.00047	0.74	0.98	F3	**GEP**
0.75	-0.00837	0.026	0.93	F1	**MARS**
0.155	20	75	0.61		**SRC**
0.92	3.2	83	0.99	F6	**GMDH**
0.88	1.8	24	0.91	F1	
0.89	1.2	73	0.98	F3	

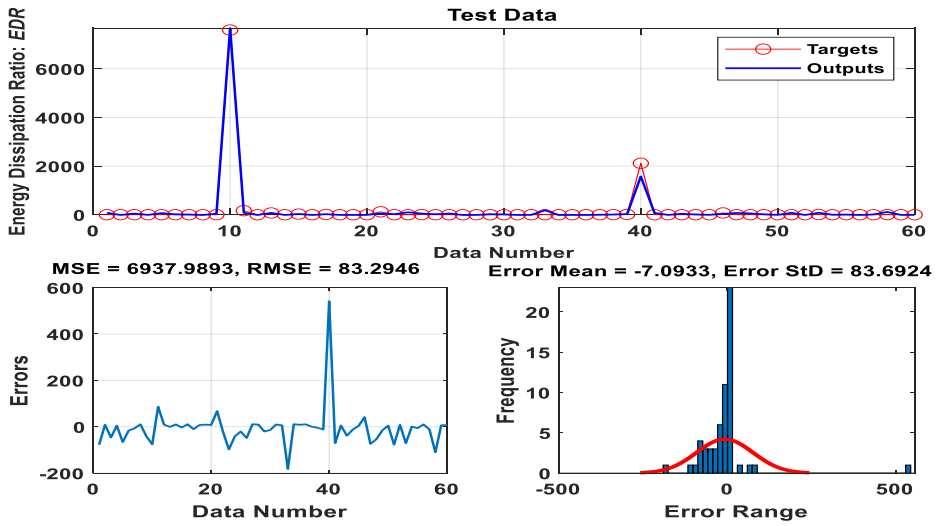

Figure 15- The output results of the GMDH model in the MATLAB environment during the test phase at the Pol Doab station.

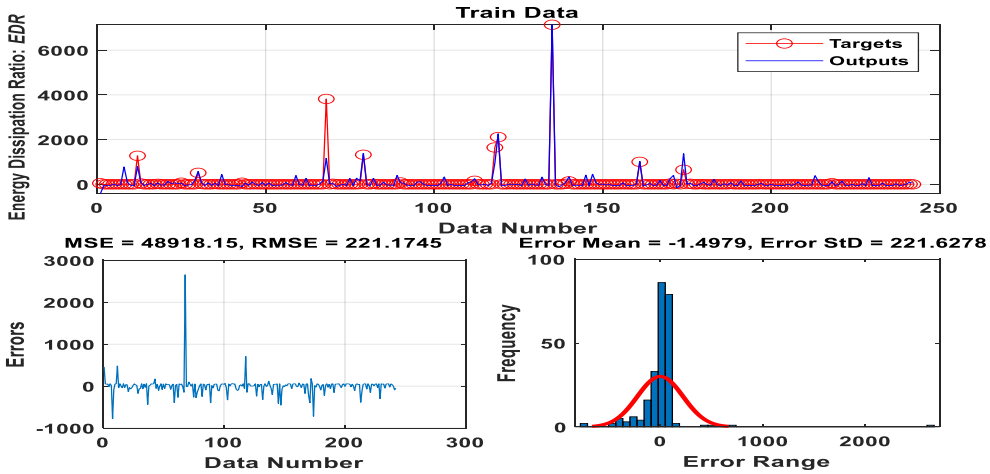

Figure 16- The output results of the GMDH model in the MATLAB environment during the training phase at the Pol Doab station.

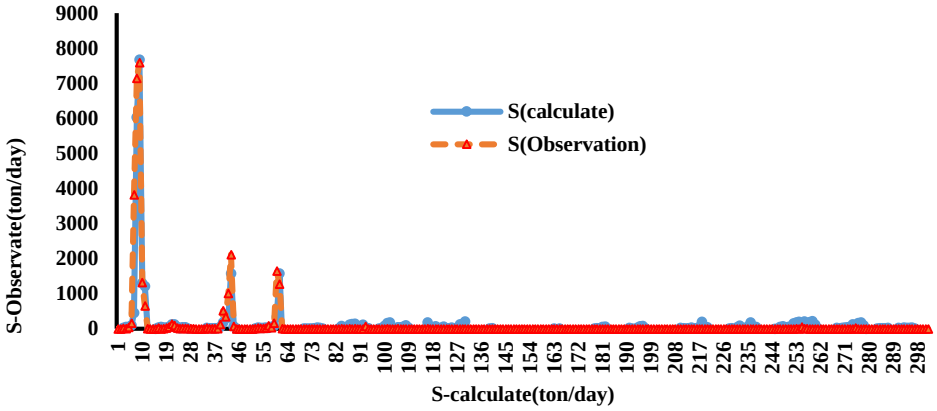

Figure 17- Visual comparison of observed and output sediment data from the GMDH model.

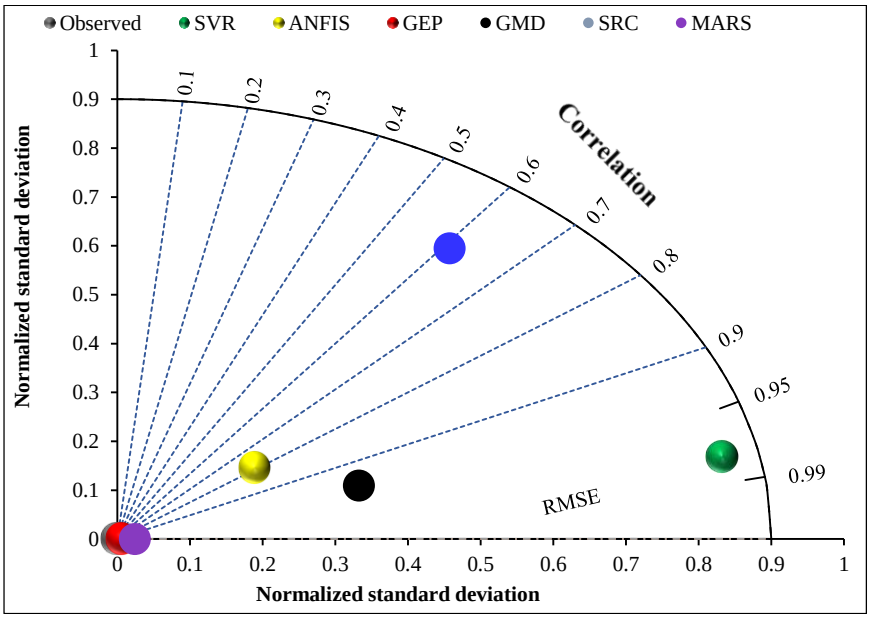

Figure 18- Comparison of the performance of the models used to estimate the suspended load with the visual method of the Taylor curve method

4. Conclusion

The findings of this study confirm the satisfactory performance of soft computing methods in predicting suspended sediment concentrations. A comparative analysis of the GMDH, GEP, ANFIS, SVR, MARS, and SRC models highlights the superior accuracy of the Gene Expression Programming (GEP) model, particularly when compared to the traditional sediment rating curve (SRC) and Verdi model number 3. The GEP model demonstrated outstanding predictive capability, achieving a high coefficient of determination (R^2) of 0.98 and a low root mean square error (RMSE) of 0.74 tons per day. These results establish the GEP model as a highly effective tool for modeling suspended sediment. All four data-driven methods—GEP, ANFIS, SVR, and MARS—outperformed the sediment rating curve in terms of estimation efficiency and accuracy, offering reliable alternatives for quantifying suspended sediment load in river systems. However, it is important to recognize that the applicability of these results may be

affected by dynamic factors such as climate change, drought, industrial development, land-use modifications, and changes in watershed morphology. Consequently, periodic model updates are essential to maintain accuracy under evolving environmental conditions. A known limitation of these models is that increasing the number of model layers or input parameters can improve accuracy but may also introduce complexity in the relationships between inputs and outputs. To address this challenge, the gamma test is recommended as a data preprocessing technique to identify the most effective combinations of input variables. Unlike many previous studies that relied on one or two variables (typically flow rate and rainfall), this study incorporated a broader range of inputs—rainfall, temperature, flow rate, and suspended sediment—enhancing the robustness of the modeling process. It is further recommended that the gamma test be used to select optimal input variables prior to model development. In addition, evaluating the predictive performance of these inputs using alternative modeling techniques—such as neuro-fuzzy systems and decision tree-based models—and comparing their results with those obtained in this study would offer valuable insights. Applying these models to other watersheds could also help generalize and validate the findings. Future research should consider incorporating additional variables beyond conventional hydrological and climatic factors (e.g., land use, vegetation cover, and soil properties) to further improve prediction accuracy. Moreover, applying meta-heuristic optimization algorithms, such as genetic algorithms, to fine-tune parameters—particularly in SVR models—can significantly enhance model performance in suspended sediment estimation. These methodological advancements contribute to the development of more accurate and reliable models, which are essential for effective water resource planning and sediment management strategies.

Author Contributions

For research articles with several authors, a short paragraph specifying their individual contributions must be provided. The following statements should be used "Conceptualization, Amir Moradinejad and Abbas Parsaie; methodology, Amir Moradinejad.; software, Amir Moradinejad.; validation, Amir Moradinejad, Abbas Parsaie., Seyed Ahmad Hosseini and Mahmoudreza Tabatabaei; formal analysis, Amir Moradinejad.; investigation, Amir Moradinejad; resources, Amir Moradinejad; data curation, Amir Moradinejad.; writing—original draft preparation, Amir Moradinejad.; writing—review and editing, Amir Moradinejad; visualization, Amir Moradinejad; supervision, Amir Moradinejad.; project administration, Amir Moradinejad.; funding acquisition, Amir Moradinejad. All authors have read and agreed to the published version of the manuscript." Please turn to the CRediT taxonomy for the term explanation. Authorship must be limited to those who have contributed substantially to the work re-ported.

All authors contributed equally to the conceptualization of the article and writing of the original and subsequent drafts.

Data Availability Statement

All data generated or analysed during this study are included in this published article [and its supplementary information files].

Ethical Considerations

The study was approved by the Ethics Committee of the Agricultural Research Education & Extention Organization (AREEO) (Ethical code: IR.UT.RES.2025.500).
The authors avoided data fabrication, falsification, plagiarism, and misconduct.

Funding

No fee was charged from anyone or anywhere for this research.
This research did not receive any specific grant from funding agencies in the public, commercial, or not-for-profit sectors.

Conflict of Interest

No one other than the authors had any role in the design of the study, in the collection, analysis, or interpretation of data, in writing the manuscript, or in the decision to publish the results.

References

Abraham, A., Steinberg, D., Philip, N. S. 2001. Rainfall forecasting using soft computing models and multivariate adaptive regression splines IEEE SMC Transactions, Special Issue on Fusion of Soft Computing and Hard.

Adamowski, J., Chan, H. F., Prasher, S. O., Sharda, V.N. 2012. Comparison of multivariate adaptive regression splines with coupled wavelet transform artificial neural networks for runoff forecasting in Himalayan micro-watersheds with limited data. *Journal of Hydroinformatics* 14(3): 731-744.

Adnan, R.M., Yaseen, Z.M., Heddam, S., Shahid, S., Sadeghi-Niaraki, A., Kisi, O. 2022. Predictability; performance enhancement for suspended sediment in rivers: Inspection of newly developed hybrid adaptive neuro-fuzzy system model. *International; Journal of Sediment Research. 37(10),* 383–398. https://doi.org/10.1016/j.ijsrc.2021.10.001.

Alizamir, M., Kisi, O., Adnan, R.M., Kuriqi, A. 2020. Modeling reference evapotranspiration by combining neuro-fuzzy and evolutionary strategies. *Acta; Geophys. 68*, 1113–1126.

Aytek, A., Kisi, O. 2008. A Genetic Programming Approach to Suspended Sediment Modeling. Journal; of Hydrology, 351: 288-298.

Azamathulla, H.M., Caun, Y.C., Aminudin, A., Chang, C. K. 2013. Suspended; sediment load prediction of river systems: GEP; approach. Arabian; Journal of Geoscience, 6: 3469-480.

Biranvand, N., Sepahvand, A. and Haqizadeh, A. 2022. Modeling of suspended sediment using machine learning algorithms in periods of low and high water (case study: Kashkan watershed). Soil; and water modeling and management, (3)2: DOI: 10.22098/mmws.2022.11262.1115

Duan, W.L.; He, B.; Takara, K.; Luo, P.P., Nover, D., Hu, M.C. 2015. Modeling suspended sediment sources and transport in the Ishikari River basin, Japan, using SPARROW, *Hydraulic Earth Systems Sciences*, 19: 1293-1306.

Eder, A.P., Strauss, T., Krueger, B., 1and, J.N., Quinton, B. 2010. A Comparative calculation of suspended sediment loads with respect to hysteresis effects (in the Petzenkirchen catchment), *Austria, Journal of Hydrology*, 389: 168-176.

Emamgolizadeh s., Bateni S. M., Shahsavani D., Ashrafi T., Ghorban H. 2015. Estimation of soil cation exchange capacity using Genetic Expression Programming (GEP) and Multivariate Adaptive Regression Splines (MARS) *Journal of Hydrology*, 529 (3), pp 1590-1600.

Ferreira C. 2001. Algorithms; for solving gene expression programming: a new adaptive problems. Complex; Systems, 13(2): 87-129.

Ikram, R.M.A., Mostafa, R.R., Chen, Z., Parmar, K.S., Kisi, O., Zounemat-Kermani, M. 2023. Water Temperature Prediction Using Improved Deep Learning Methods through Reptile Search Algorithm and Weighted Mean of Vectors Optimizer; *J. Mar. Sci. Eng. 11*, 259. https://doi.org/10.3390/jmse11020259.

Ivakhnenko, A.G. 1976. The Group Method of Data Handling in Prediction Problems, Soviet Automatic Control of Avtomotika, 9: 21-30.

Keshtegar, B., Piri, J., Hussan, W.U., Ikram, K., Yaseen, M., Kisi, O., Adnan, R.M., Adnan, M., Waseem, M. 2023. Prediction of Sediment Yields Using a Data-Driven Radial M5 Tree Model. *Journal; of Water 2023*, 15, 1437. https://doi.org/10.3390/w15071437;

Kisi, O., Ozkan, C., Bahriye, A. 2012. Modeling; Discharge-Sediment Relationship Using Neural Networks with Artificial Bee Colony Algorithm, Journal of Hydrology, 428-429: 94-103.

Mehrizi Haeri, AA. 2012. Data mining: concepts, methods, and applications. Master's; thesis in economic and social statistics, Faculty of Economics, Allameh Tabatabai University.

Melesse, A. M., Ahmad, S., McClain, M. E., Wang, X. and Lim, Y.H. 2011. Suspended; sediment load prediction of river systems: an artificial neural network approach. Agriculture; Water Management, 98: 855–866.

Moradinejad, A. 2024. Suspended load modeling of river using soft computing techniques. *Water Resources Management*. Advance online publication. https://doi.org/10.1007/s11269-023-03722-7.

Moradinejad, A., Khosrobeigi, S., Akbari, M., Hosseini, SA. 2024. Investigating soft calculation methods in river suspended sediment estimation (Hassan Abad station of Tirah river). *Water and Soil Management and Modeling*, *4*(2), 241-260. DOI: 10.22098/mmws.2023.12620.1258

Mostafa, R.R., Kisi, O., Adnan, R.M., Sadeghifar, T., Kuriqi, A. 2023. Modeling Potential Evapotranspiration by Improved Machine Learning Methods Using Limited Climatic Data. *Water*; *15*, 486. https://doi.org/10.3390/w15030486;

Satari, M.T., Rezazadeh Jodi, A., Safdari, F., Kahramanzadeh, F. 2016. Performance evaluation of M5 tree model and support vector regression methods in river suspended sediment modeling. Protection; of water and soil resources, (1) 6, https://civilica.com/doc/1297623.

Tayfur, G. 2012. Soft; computing in water resources engineering: Artificial neural networks, fuzzy logic and genetic algorithms. *WIT; Press; Dorset.*

Walling, D. E., Webb, B. W. 1988. The reliability of rating curve estimates of suspended sediment yield: some further comments. *Sediment; Budgets (Proceedings of the Porto Alegre Symposium)*, (174), 337–350.

Yeganeh-Bakhtiary, A., Eyvazoghli, H., Shabakhty, N., Kamranzad, B., Abolfathi, S. 2022. Machine; Learning as a Downscaling Approach for Prediction of Wind Characteristics under Future Climate Change Scenarios. *Complexity; 13*, 8451812. https://doi.org/10.1155/2022/8451812.Abolfathi, S., Yeganeh

Yilmaz, B., E. Aras, Nacar, S., Kankal, M. 2018. Estimating suspended sediment load with multivariate adaptive regression spline, teaching-learning based optimization, and artificial bee colony models. *Sci Total Environ* 639:826–840. https://doi.org/10.1016/j.scitotenv.2018.05.153.

Zhang, W., Goh, A.T.C. 2016. Multivariate adaptive regression splines and neural network models for prediction of pile drivability. *Geosci Front* 7:45–52. https://doi.org/10.1016/j.gsf.2014.10.003

Sadegh Safar, M. J. 2020. Hybridization of multivariate adaptive regression splines and random forest models with an empirical equation for sediment deposition prediction in open channel flow. *Journal Pre-proofs*, S0022-1694(20)30852-0, https://doi.org/10.1016/j.jhydrol.2020.125392.

García-Nietoa, P.J., E. García-Gonzaloa, J.R. Alonso Fernándezb, C. Díaz Muñizb. 2019. Modeling algal atypical proliferation using the hybrid DE–MARS–basedapproach and M5 model tree in LaBarca reservoir: A case study in northernSpain. *Journal homepage*.

Sultani, W., Chen, C., Shah, M. 2018. Real-World Anomaly Detection in Surveillance Videos. In *Proceedings of the IEEE/CVF Conference on Computer Vision and Pattern Recognition (CVPR)*.

Koza, J. R. 1992. *Genetic Programming: On the Programming of Computers by Means of Natural Selection*. MIT Press.

Russel, SO., Campbell, PF. 1996. Reservoir operating rules with fuzzy programming. J Water Resour Plan Manag 122(3):165–170.